Parametric Amplification and Generation of Surface Acoustic Waves on a Monolithic MIS Structure

doi: 10.1063/1.90530

samples of tungsten carbide in silicon nitride showed up in microfocus x-ray measurements but behaved like vacancies acoustically. When they were lapped down, the tungsten carbide was found to be supported from the surrounding medium only by a small fillet.

Finally, this high-frequency technique appears to yield information on the uniformity of the inclusion. In one case where a two-phase material was present, scattered signals from within the inclusion were clearly observed.

[1]B. T. Khuri-Yakub and G. S. Kino, Appl. Phys. Lett. 30, 78 (1977).
[2]G. S. Kino, J. Appl. Phys. 49, 3190 (1978).

Parametric amplification and generation of surface acoustic waves on a monolithic MIS structure

S. Minagawa

Clarion Co., Kamitoda, Toda, Saitama, Japan

T. Kugaya, K. Tsubouchi, and N. Mikoshiba

Research Institute of Electrical Communication, Tohoku University, Katahira, Sendai, Japan
(Received 15 May 1978; accepted for publication 27 June 1978)

We report on a new surface-acoustic-wave (SAW) amplifier and generator on a monolithic MIS structure with a uniform pump electrode. The gain for the forward SAW and the generation of the backward SAW have been observed in an Al/ZnO/SiO_2/Si structure. Using the same structure, we observed for the first time the parametric generation of SAW of 222 MHz by the uniform pumping, even if there is no signal input.

PACS numbers: 43.88.Lc, 72.50.+b, 73.40.Qv, 43.60.+d

As is well known, one of the merits of the SAW parametric amplifier compared with the usual traveling-wave-type amplifier is that this device can be operated, in principle, without Joule heating. Various types of SAW parametric amplifiers have been investigated since 1970.[1-3] However, the configurations where the signal and pump waves are simultaneously propagated in the same direction[2,3] or where the interdigital pump electrode is fabricated on the SAW propagation path[1] have the following weak points. In the former type, a rather high pump power is required, so that the energy of pump waves is distributed over harmonic components. Also, a difficult fine fabrication of the pump transducer is required since the pump frequency ω_p is higher than the signal frequency ω_s. In the latter type, the bandwidth is relatively narrow and fixed and the parametric amplifier of external diode is required.

On the other hand, as an inverse process of the convolution, Yamanishi *et al.*[4] proposed a configuration where the semiconductor is placed closely to the air gap on the piezoelectric substrate and the semiconductor is pumped uniformly, i.e., $\omega_p = 2\omega_s$, and $\beta_p = 0$, β_p being the propagation constant of the pump wave. However, they could not clearly demonstrate the parametric amplification of the SAW, since they used a separated-medium configuration where the nonlinear interaction seems to be weak and they could not estimate the proper threshold pumping voltage because of the ambiguity about the nature of nonlinearity at that time.

In this paper, we propose and experimentally demonstrate a new parametric amplifier and generator of SAW on a monolithic MIS structure with a uniform pump electrode. A schematic configuration of the SAW parametric amplifier on an Al/ZnO/SiO_2/Si (MIS) structure is shown in Fig. 1.

In the MIS structure, the parametric interaction occurs between a propagating potential of SAW (ω) generated by an interdigital transducer and the uniform pump potential (2ω) applied to the center electrode by the nonlinearity of the capacitance of the space-charge layer in Si.[5] Thus, we can expect that the forward wave is amplified, and simultaneously the backward wave is generated as an idler wave. Moreover, we can expect theoretically that if the pump power is larger than a threshold value, the generation of SAW propagating to the right and left occurs even if there is no signal input.[6]

We used the sample which consists of a thermally oxidized (in dry O_2) expitaxial n-on-n^+ silicon (thickness and resistivity of the expitaxial layer are 9 μm and 90 Ω cm, respectively, thickness of the oxide layer $=1000$ Å, thickness of n^+ Si $=0.3$ mm) and a dc-sputtered layer of ZnO (thickness $=6$ μm). The aluminum elec-

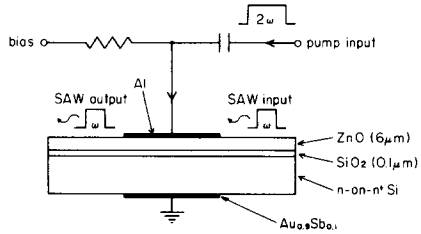

FIG. 1. A schematic configuration of the SAW amplifier and generator on an Al/ZnO/SiO_2/Si (MIS) structure.

 0003-6951/78/3308-0687$00.50

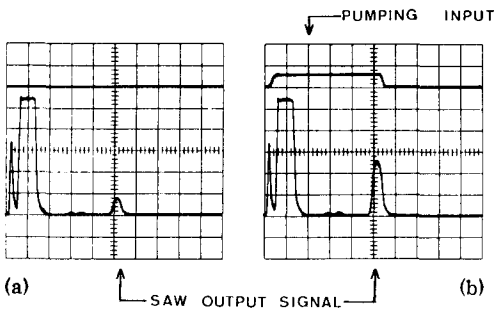

FIG. 2. Parametric amplification of the forward wave. Upper trace: (a) no pumping power; (b) pumping power = 34.9 dBm (f_{pump} = 444 MHz). Lower trace: SAW output signal (f_{SAW} = 222 MHz). Horizontal scale: 2 μs/div.

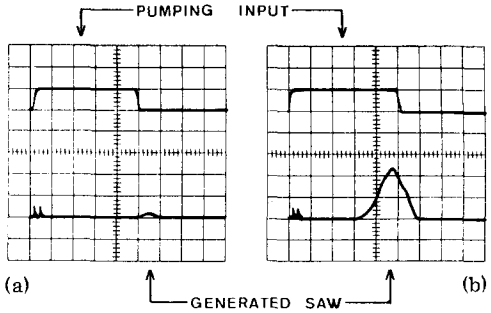

FIG. 4. SAW parametric generation by the uniform pumping of center electrode without SAW signal input. Upper trace: pumping power (f_{pump} = 444 MHz) (a) at 36.4 dBm; (b) 39.1 dBm. Lower trace: SAW signal at the input transducer (f_{SAW} = 222 MHz). Horizontal scale; 5 μs/div.

trode (dimension = 2×15 mm²) was deposited at the center of the sample. The back Ohmic contact was evaporated with $Au_{0.9}Si_{0.1}$. Two aluminum transducers corresponding to the SAW wavelength of 12 μm were deposited on both sides of the center electrode (the two-port insertion loss was 55 dB). The experiment was carried out for the signal SAW of ω_s = 222 MHz and the pump power of ω_p = 444 MHz.

Figures 2(a) and 2(b) show an example of the observed parametric amplification of the forward wave under the condition of pulse-mode operation. In Figs. 2(a) and 2(b) the upper and lower traces show the waveform of the pumping voltage and the output signal of the forward wave. In Fig. 2(a) no pumping voltage is applied. The pumping power is 34.9 dBm in Fig. 2(b). We could observe the gain of about 10 dB in this case. The dc bias applied to the center electrode can be used to change the surface potential of Si and then change the strength of the nonlinear interaction. We observed the peak amplification when the Si surface is weakly depleted from the flatband. This is consistent with the theoretical consideration.[5]

Figures 3(a) and 3(b) show an example of the generation of the backward wave observed at the input transducer under the same experimental condition as that in Fig. 2. In Fig. 3(a), when no pumping power is applied, no backward wave is observed. When there is pumping power, the backward wave is generated as shown in Fig. 3(b). In an ideal case, we expect a uniform output of the backward wave until about 12 μs, since the

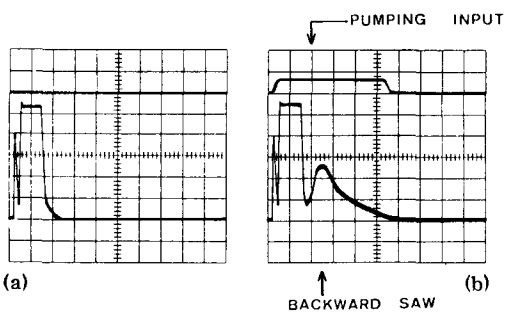

FIG. 3. Parametric generation of the backward wave. Upper trace: (a) no pumping power; (b) pumping power = 34.9 dBm (f_{pump} = 444 MHz). Lower trace: SAW signal at the input transducer (f_{SAW} = 222 MHz). Horizontal scale: 2 μs/div.

transit times of SAW from the input transducer to the edge of the center electrode and over the length of the center electrode are about 1 and 5 μs, respectively. However, as shown in Fig. 3(b), we observed the decreasing tail of the backward wave which seems due to the propagation loss. The generation of the backward wave clearly shows that the amplification of the forward wave is not the decrease of loss but really the parametric amplification.

We show for the first time in Fig. 4 the experimental results of parametric generation of SAW observed at the input transducer by the uniform pumping of center electrode, even if there is no signal input. Since there is a possibility that bulk waves are also generated at the center electrode, we confirmed by the test that the observed signal is due to the SAW, i.e., we found that the signal disappeared when an acetone drop was put on the surface between the electrode and the transducer.

Figures 4(a) and 4(b) show the waveforms of SAW in the cases of low (36.4 dBm) and high (39.1 dBm) pumping powers. We estimate from Figs. 4(a) and 4(b) that the build-up times required for the parametric generation of SAW are about 4 [in Fig. 4(a)] and 3 [in Fig. 4 (b)] times the transit time of SAW over the length of the center electrode, respectively. This result indicates the general trend of the decrease of build-up time with the increase of pumping power. We found also that the parametric generation of SAW cannot be observed with the pumping pulse width less than 15 μs. In the present experiment, the output power of SAW was −34 dBm when the pumping power was 37 dBm. Therefore, we estimate that the conversion efficiency from the pumping to the SAW power is −44 dB, taking the insertion loss (27 dB) of the transducer into account.

In conclusion, we have demonstrated (1) the parametric amplification of the forward SAW and the generation of the backward SAW and (2) the parametric generation of SAW without an input SAW signal, in the MIS structure. This device can be used as a tunable and wide-band frequency transducer of SAW without microfabrication and has wide potential applications.

[1]G. Chao, Appl. Phys. Lett. 16, 399 (1970).
[2]Y. Nakagawa, K. Yamanouchi, and K. Shibayama, Trans. Inst. Electron. Commun. Jn. 55-A, 377 (1972).

[3]J. Wolter, Phys. Lett. A 42, 115 (1972).
[4]M. Yamanishi, T. Kawamura, S. Takada, and N. Mikoshiba, Report of Applied Electron Physics Section, the Japan Society of Applied Physics, No. 362, 1975 (in Japanese) (unpublished).
[5]K. Tsubouchi, S. Minagawa, and N. Mikoshiba, J. Appl. Phys. 47, 5187 (1976).
[6]S. Minagawa, T. Kugaya, K. Tsubouchi, and N. Mikoshiba, 1977 *Ultrasonics Symposium Proceedings, Phoenix*, IEEE 77 CH 1264-1SU (IEEE, New York, 1977), p. 629.

Surface segregation in $LaNi_5$ induced by oxygen

Th. von Waldkirch and P. Zürcher

Laboratory of Solid State Physics, ETH Hönggerberg, 8093 Zürich, Switzerland
(Received 3 July 1978; accepted for publication 16 August 1978)

LEED and AES studies of $LaNi_5$ single crystals cleaved in UHV and exposed to oxygen and hydrogen show that surface segregation of La is induced at room temperature by oxygen, but not by hydrogen. This segregation is driven by the chemical exchange reaction (La-Ni)+O→(La-O)+Ni. A surface-layer model is derived supporting the important implications of the segregation for the excellent kinetics in hydrogenation and the resistance to contaminants.

PACS numbers: 68.20.+t, 64.75.+g, 82.65.Nz, 81.60.Bn

Due to their ability to store reversibly large amounts of hydrogen—a promising energy carrier of the future—some intermetallic compounds have gained high interest in the last few years.[1–3] $LaNi_5$ is especially promising because it shows large hydrogen capacity together with good kinetics and high resistance against contamination.[1,4] While extensive studies exist on bulk features,[5,6] the nature of the surface has so far obtained little attention only. However, activated $LaNi_5$ is a fine powder, and its surface therefore represents an important factor in the hydriding process. Very recently, the first surface study on polycrystalline $LaNi_5$ samples by XPS and magnetic measurements was presented.[7] The air-exposed samples revealed an abundant lanthanum content of the surface in oxide or hydroxide form together with metallic nickel precipitations which increased with the number of hydrogenation cycles. This effect was recognized as a self-restoring mechanism of the active surface, since metallic nickel is—like other transition metals—known to be capable of splitting the hydrogen molecule.[8]

Surface segregations in intermetallic compounds are not new.[9] The one found in $LaNi_5$,[7] however, is of special interest, since it is related to the excellent hydriding properties of this compound. We present the first Auger electron spectroscopy (AES) and LEED investigations of $LaNi_5$ single crystals, cleaved in an ultrahigh vacuum (UHV) of 6×10^{-10} Torr, which characterize the mechanism of this segregation more precisely.

The single crystals were prepared from 99.9% pure La (Res. Chem.) and 99.999% pure Ni (Koch Light) in UHV by the Czochralski method (10). The rod-shaped crystals could easily be cleaved in UHV, producing an uncontaminated yet not plane-shaped surface. The AES spectra were taken on a cylindrical mirror spectrometer with a retarding field analyzer. The primary energy used was 2000 eV. La exhibits pronounced AES peaks at 78 eV ($N_3N_{4,5}O_{2,3}$) and 59 eV ($N_3N_{4,5}O_1$) kinetic energy, and a Ni peak at 61 eV ($M_{2,3}M_{4,5}M_{4,5}$).[11] The latter two lines are not resolved and must, after baseline correction, be separated by computer simulation. Since the mean free path, i.e., the probing depth, of the 59-, 61-, and 78-eV electrons are practically the same (~5 Å),[12] the peak-to-peak height (h_{pp}) of the La (78-eV) line determines that of the La (59-eV) line.[11,12] Hence, h_{pp} (Ni[61 eV]) can be calculated from the experimental baseline-corrected value of the overlapping La/Ni line by simulated subtraction of the La (59-eV) peak. The comparison of standard spectrum h_{pp}^{st}(Ni)/h_{pp}^{st}(La) ratios[11] with those measured is a means to determine the Ni/La concentration ratio C_{Ni}/La of the $LaNi_5$ surface,[13]

$$C_{Ni/La}=\frac{h_{pp}^{st}(La[78\ eV])}{h_{pp}^{st}(Ni[61\ eV])}\,\frac{h_{pp}^{exp}(Ni[61\ eV])}{h_{pp}^{exp}(La[78\ eV])}. \tag{1}$$

The ratio of escape depths, the ratio of the backscattering factors, and the total number of atoms per unit volume may yield systematic errors to $C_{Ni/La}$ determined from Eq. (1).[13] Application of Eq. (1) to the present data results in $C_{Ni/La}\simeq 4.65$ immediately after cleavage. The small difference to the stoichiometric value of 5 shows that these errors are below 10%. Since the linewidths remain unchanged during the experiment within the experimental uncertainty, the systematic errors can be assumed as fixed. Thus, they have no influence on relative changes dealt with in this paper.

Besides La and Ni, the 510-eV line of oxygen (KL_2L_2) and the 273-eV line of carbon (KL_2L_2) were monitored. The probing depth at this energy is about twice that for La and Ni.

After cleavage, a well-defined LEED pattern indicated a crystalline surface structure. The surface was then exposed to 3 and 10 L (1 L = 10^{-6} Torr sec) of 99.998% pure oxygen. During the second exposure, the LEED pattern disappeared. The AES measure-

 0003-6951/78/3308-0689$00.50